nature microbiology

SUPPLEMENTARY INFORMATION

https://doi.org/10.1038/s41564-019-0455-0

In the format provided by the authors and unedited.

Microfluidic-based transcriptomics reveal force-independent bacterial rheosensing

Joseph E. Sanfilippo[1,6], Alexander Lorestani[1,6], Matthias D. Koch[1,2], Benjamin P. Bratton[1,2], Albert Siryaporn[1,3,4], Howard A. Stone[5] and Zemer Gitai[1*]

[1]Department of Molecular Biology, Princeton University, Princeton, NJ, USA. [2]Lewis-Sigler Institute for Integrative Genomics, Princeton University, Princeton, NJ, USA. [3]Department of Physics and Astronomy, University of California, Irvine, Irvine, CA, USA. [4]Department of Molecular Biology and Biochemistry, University of California, Irvine, Irvine, CA, USA. [5]Department of Mechanical and Aerospace Engineering, Princeton University, Princeton, NJ, USA. [6]These authors contributed equally: Joseph E. Sanfilippo, Alexander Lorestani. *e-mail: zgitai@princeton.edu

Supplementary Information for

Microfluidic-based transcriptomics reveal force-independent bacterial rheosensing

Joseph E. Sanfilippo[a,1], Alexander Lorestani[a,1] Matthias D. Koch[a,b], Benjamin P. Bratton[a,b], Albert Siryaporn[a,c,d], Howard A. Stone[e], Zemer Gitai[a,2]

[a]Department of Molecular Biology, Princeton University, Princeton, NJ 08544
[b]Lewis-Sigler Institute for Integrative Genomics, Princeton University, Princeton, NJ 08544
[c]Department of Molecular Biology and Biochemistry, University of California, Irvine, Irvine, CA 92697
[d]Department of Physics and Astronomy, University of California, Irvine, Irvine, CA 92697
[e]Department of Mechanical and Aerospace Engineering, Princeton University, Princeton, NJ 08544

[1]These authors contributed equally.
[2]To whom correspondence should be addressed. Email: zgitai@princeton.edu

This includes:
Supplementary Figures 1 to 11
Supplementary Tables 3 to 5
Supplementary references

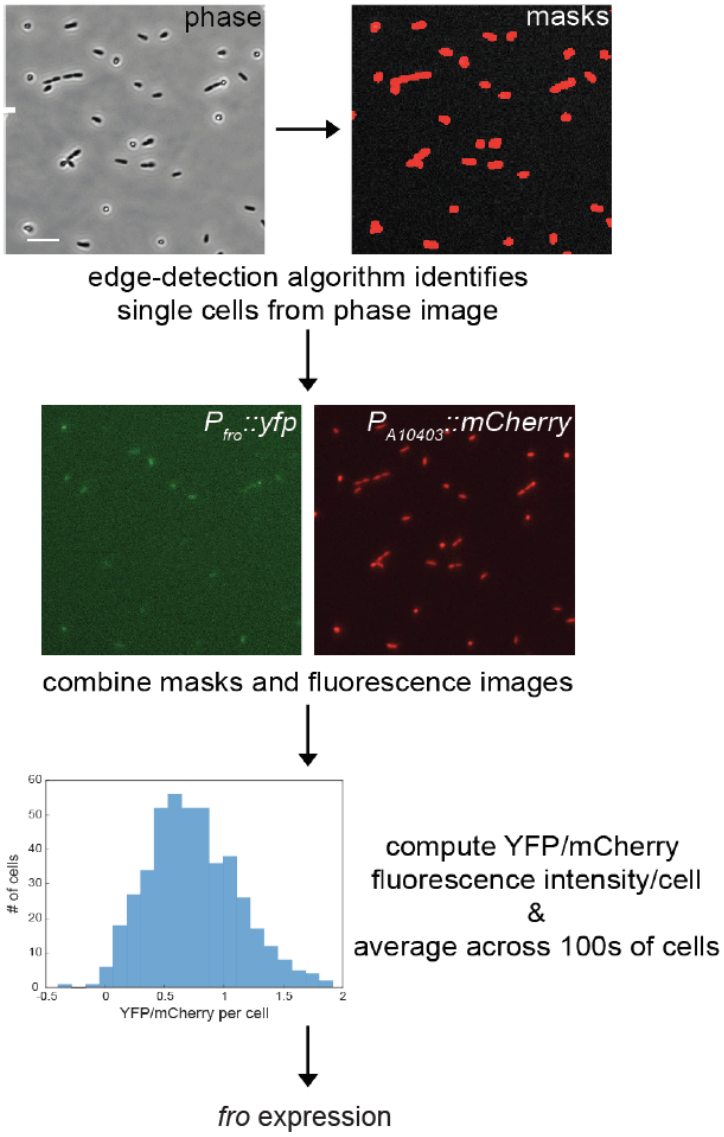

Supplementary Figure 1: Image analysis pipeline for quantification of *fro* expression. First, an edge detection algorithm is applied to phase contrast images to build cell masks. Then, the fluorescence within each mask is measured from the corresponding YFP and mCherry images. Scale bar indicates 5 μm. The YFP/mCherry fluorescence ratio per cell is computed and averaged across hundreds of cells. *fro* expression is represented as the population's average cellular YFP/mCherry ratio.

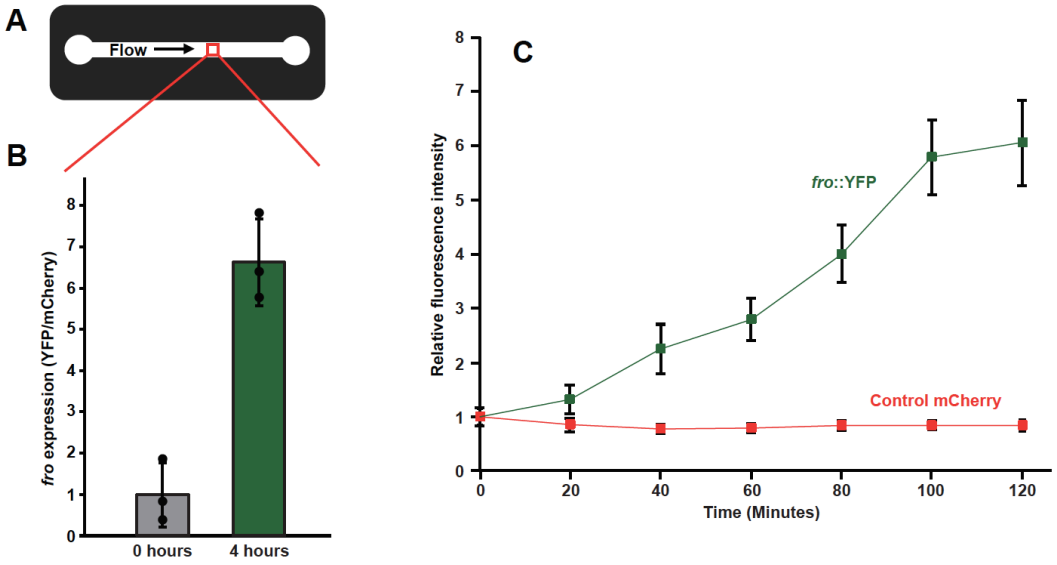

Supplementary Figure 2: Flow induces *fro* expression approximately 7-fold. (A) Schematic depicting the view from above the microchannel used in B. These channels are 50 μm tall by 500 μm wide. (B) *fro* expression of cells before flow (0 hours) and after 4 hours of flow (4 hours) at a shear rate of 800 sec^{-1}. *fro* expression at 0 hours was set to 1. Raw images shown in Figure 1E. Error bars show SD of three independent replicates and points indicate values for each replicate. (C) Fluorescence intensity of YFP channel (in green) and mCherry channel (in red) for cells exposed to a shear rate of 800 sec^{-1}. YFP and mCherry intensity at 0 minutes set to 1. Error bars represent the SEM of 30 cells for each data point.

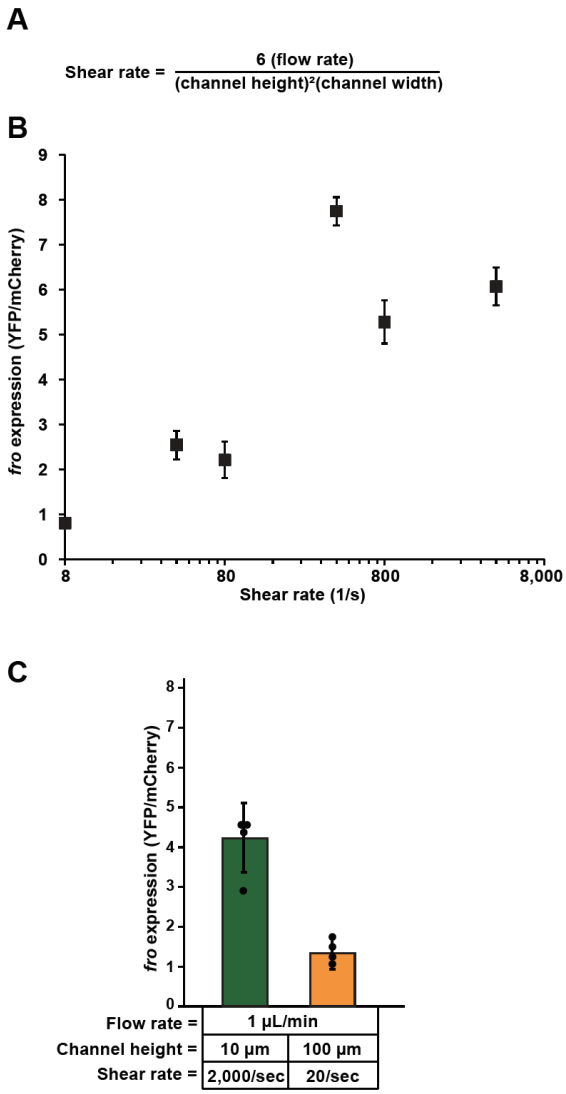

Supplementary Figure 3: Shear rate tunes *fro* expression. (A) Equation showing the relationship between shear rate, flow rate and channel dimensions. (B) *fro* expression after cells were subjected to flow at shear rates of 8-4,000 sec^{-1} (flow rates ranging from 0.1 to 50 µl/min) in a 50 µm tall channel for 2 hours. (C) *fro* expression after cells were subjected to flow at shear rates of 2,000 sec^{-1} or 20 sec^{-1} (channel heights of 10 µm or 100 µm) at a flow rate of 1 µl/min for 2 hours. *fro* expression in 10 µm or 100 µm tall channels are significantly different with P=0.005, calculated by a 2-sided T-test. *fro* expression is quantified by the ratio of YFP to mCherry fluorescence across a population of single cells. *fro* expression with no flow was set to 1. Error bars in B represent SEM of three independent replicates. Error bars in C represent SD of four independent replicates.

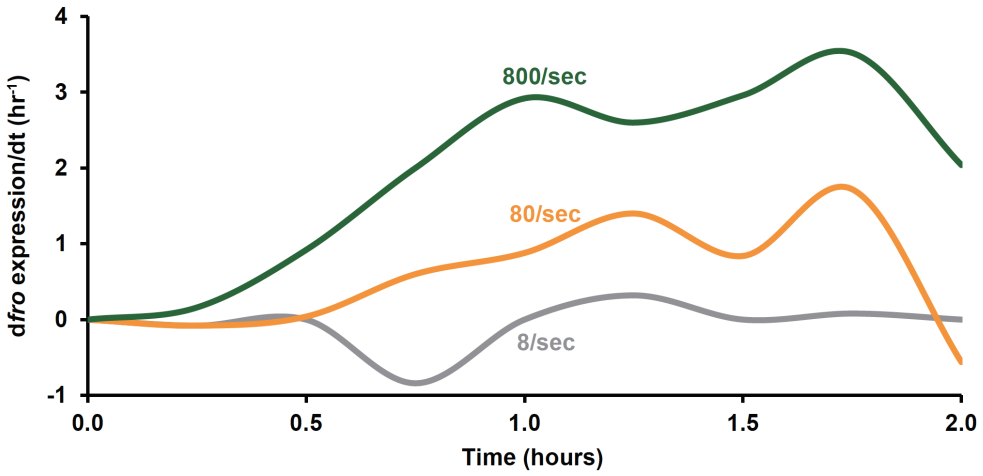

Supplementary Figure 4: Shear rate tunes *fro* induction kinetics. The first derivative of the *fro* induction curve presented in Fig. 2B, calculated by the change in *fro* expression (d*fro* expression) divided by change in time (dt). The derivative is represented in change per hour. The data presented is an average of three independent replicates. *fro* expression for this experiment was measured over 2 hours of time in the presence of 8 (gray line), 80 (yellow line), and 800 sec^{-1} (green line) shear rates.

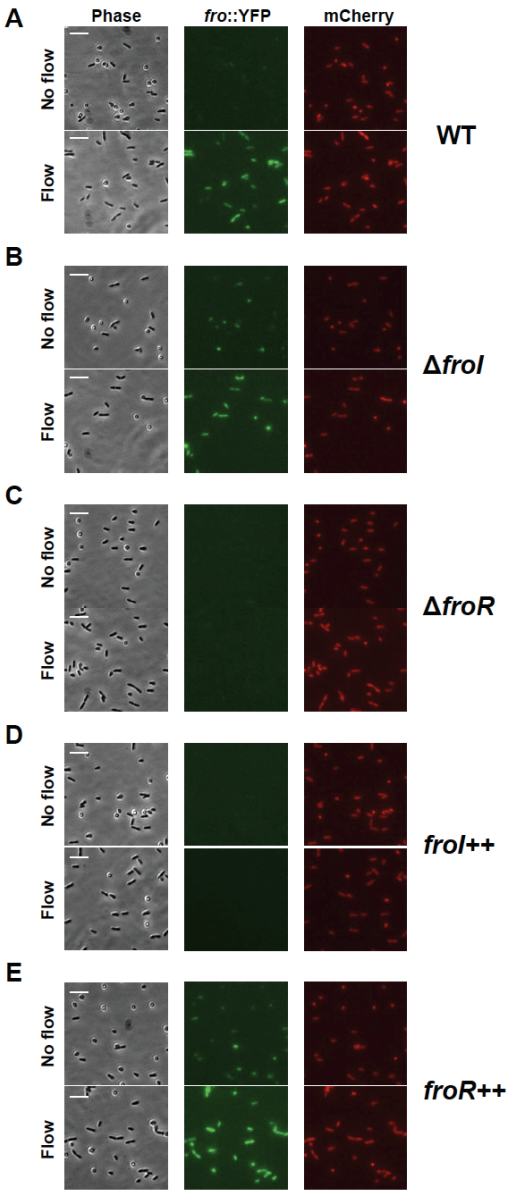

Supplementary Figure 5: The sigma factor FroR and anti-sigma factor FroI regulate *fro* expression. (A-E) Images of cells either before flow (No flow) or after being exposed to flow (Flow) at a shear rate of 800 sec^{-1} for 120 min. Left images show the phase contrast channel, middle images show the YFP channel, and right images show the mCherry channel. All strains have the *fro*::YFP reporter and a constitutively expressed mCherry reporter. (A) shows wild-type (WT) cells, (B) shows a Δ*frоI* mutant, (C) shows a Δ*froR* mutant, (D) shows a *frоI*++ overexpression strain, and (E) shows a *froR*++ overexpression strain. Scale bars indicate 5 μm. Images are representative of three independent replicates.

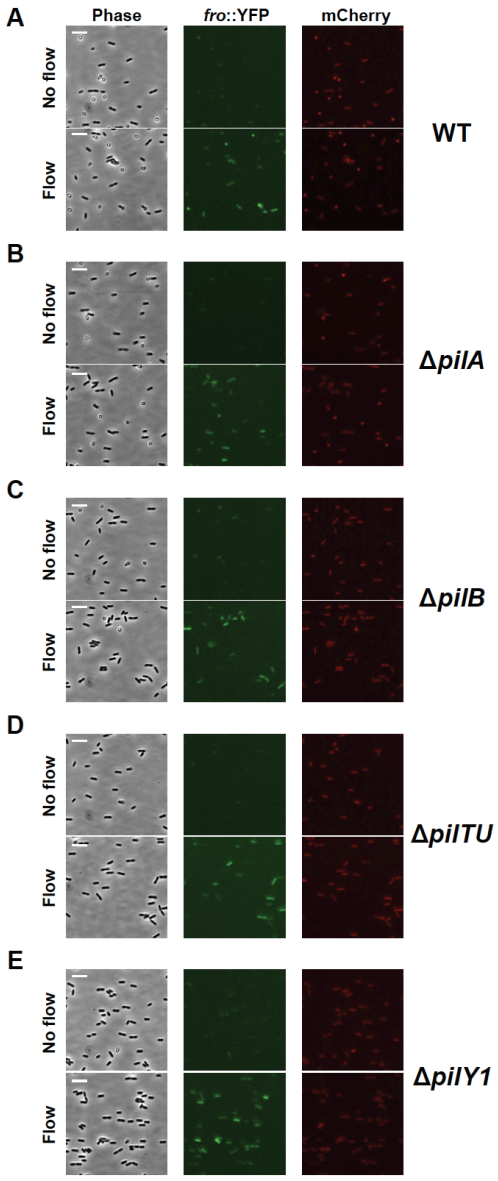

Supplementary Figure 6: Known bacterial surface sensors do not regulate *fro* expression. (A-E) Images of cells either before flow (No flow) or after being exposed to flow (Flow) at a shear rate of 800 sec^{-1} for 120 min. Left images show the phase contrast channel, middle images show the YFP channel, and right images show the mCherry channel. All strains have the *fro*::YFP reporter and a constitutively expressed mCherry reporter. (A) shows wild-type (WT) cells, (B) shows a Δ*pilA* mutant, (C) shows a Δ*pilB* mutant, (D) shows a Δ*pilTU* mutant, and (E) shows a Δ*pilY1* mutant. Scale bars indicate 5 μm. Images are representative of three independent replicates.

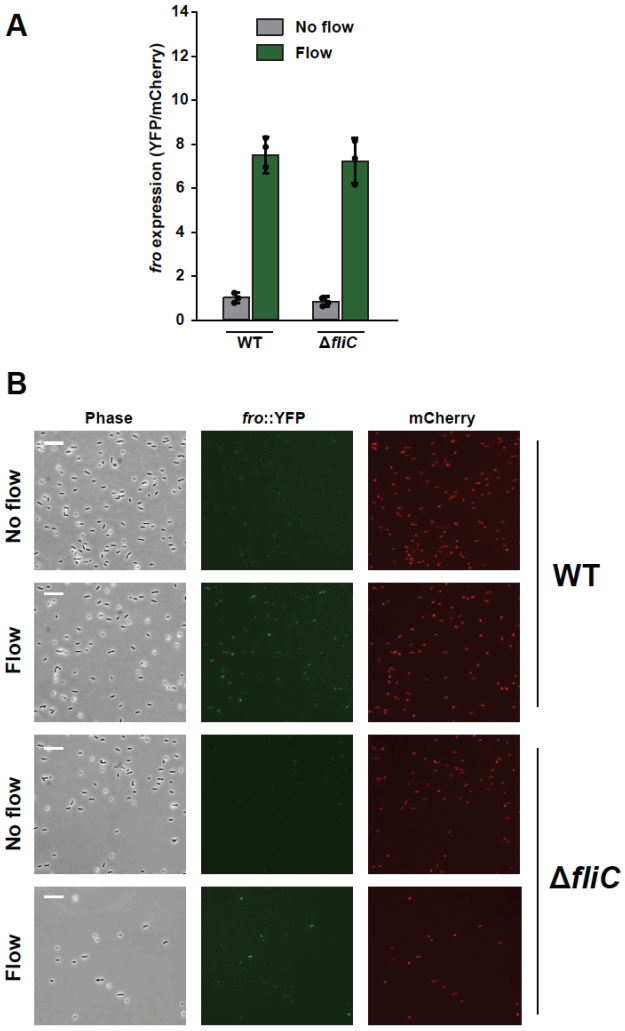

Supplementary Figure 7: The flagellum is not required for *fro* induction. (A) *fro* expression levels in wild-type cells and Δ*fliC* mutant cells either subjected to no flow (gray bars) or 2 hours of flow at a shear rate of 400 sec^{-1} (green bars). *fro* expression in no flow for WT is normalized to 1. Error bars show SD of three independent replicates and points indicate values for each replicate. Channels used these experiments were 50 μm tall by 500 μm wide. (B) Images of WT and Δ*fliC* mutant cells either before flow (No flow) or after being exposed to flow (Flow) at a shear rate of 800 sec^{-1} for 2 hours. Left images show the phase contrast channel, middle images show the YFP channel, and right images show the mCherry channel. Scale bars indicate 10 μm. Images are representative of three independent replicates.

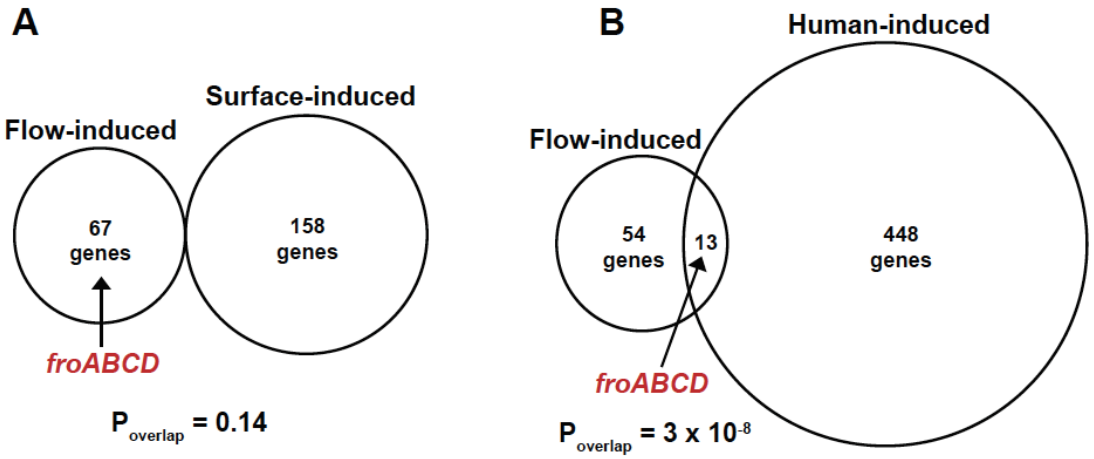

Supplementary Figure 8: The flow-induced transcriptome is distinct from the surface-induced transcriptome and includes genes induced during human infection. (A) Overlap of flow-induced genes at 4 hours and surface-induced genes from (*16*). (B) Overlap of flow-induced genes at 4 hours and genes induced at least 3-fold during human infection from *(25)*. *froABCD* genes are induced by flow and human infection, but not by surface attachment. P-values were calculated using the hypergeometric distribution and represent the likelihood that the overlap of datasets is due to chance.

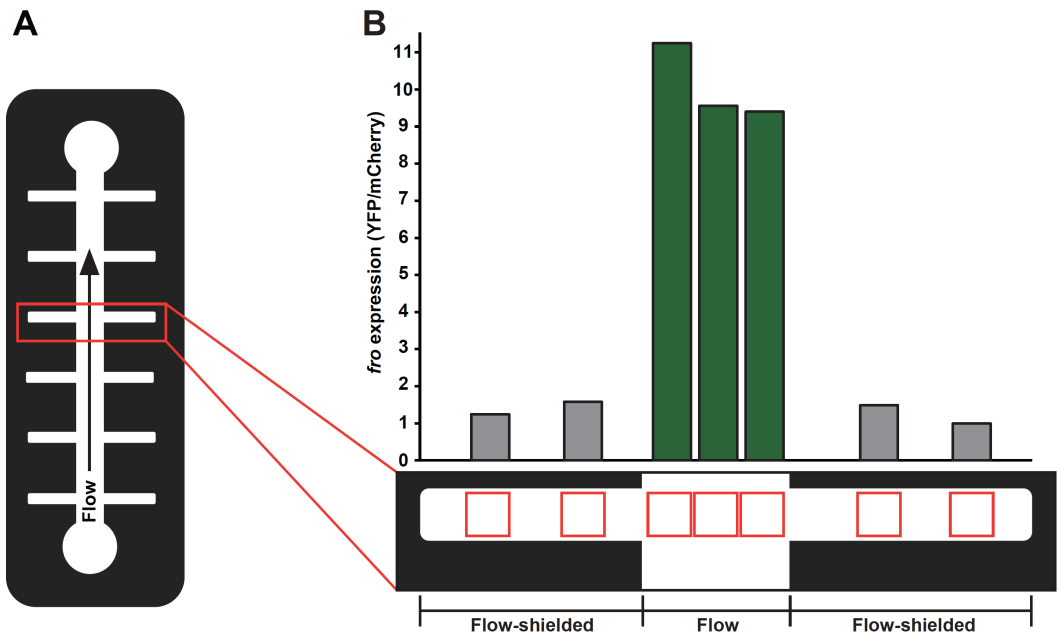

Supplementary Figure 9: Surface attached cells in flow-shielded regions of a channel do not induce *fro* expression. Schematic depicting the view from above the microchannel used with flow-shielded inlets. These channels are 50 μm tall by 500 μm wide. (B) Quantification of *fro* expression from cells at different positions along the channel after 4 hours of flow at a shear rate of 800 sec^{-1}. Raw images shown in Figure 4B. The 7 bars on the graph correspond to quantification of cells found in locations of the 7 red squares shown in the schematic below the bar graph. The schematic is a zoomed in portion of A highlighted with the red square. *fro* expression of cells before flow treatment is set to 1.

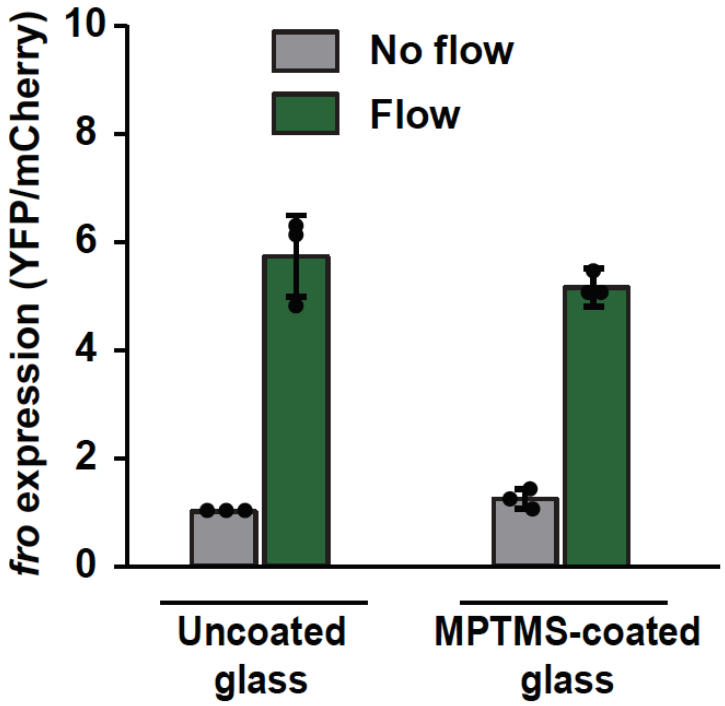

Supplementary Figure 10: Rheosensing is not affected by thiol coating of the channel surface. Quantification of *fro* expression from wild-type cells in uncoated channels or channels coated with MPTMS (3-Mercaptopropyl trimethoxysilane). MPTMS was previously shown to increase adhesion between *P. aeruginosa* and the channel surface (20). Cells before (gray) or after (green) 2 hours of flow at a shear rate of 800 sec^{-1}. *fro* expression for WT no flow was set to 1. Error bars show SD of three independent replicates and points indicate values for each replicate.

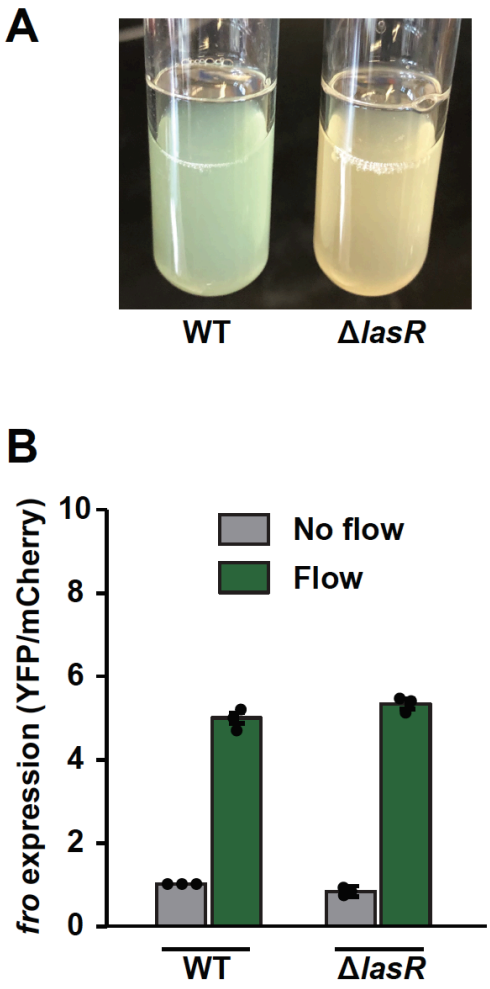

Supplementary Figure 11: Rheosensing is not controlled by canonical quorum sensing. (A) Color phenotypes of cell cultures showing wild-type (WT) cells with blue-green color due to phenazines and Δ*lasR* mutant cells lacking pigments. (B) Quantification of *fro* expression from wild-type and Δ*lasR* mutant cells in no flow (gray) or after 2 hours of flow at a shear rate of 800 sec^{-1} (green). *fro* expression for WT no flow was set to 1. Error bars show SD of three independent replicates and points indicate values for each replicate.

Table S3. Strains used in this study.

Strain	Description	Reference
E. coli		
S17-1	wild-type; used for cloning and conjugation	(*33*)
P. aeruginosa		
PA14	wild-type; clinical isolate from a burn wound	(*34*)
AL143	PA14 *fro::yfp attB*::[$P_{A1/04/03}$-*mCherry*]	This study.
AL297	PA14 *fro::yfp attB*::[$P_{A1/04/03}$-*mCherry*] Δ*pilA aacc1*::FRT	This study.
AL180	PA14 *fro::yfp attB*::[$P_{A1/04/03}$-*mCherry*] Δ*pilB aacc1*::FRT	This study.
AL169	PA14 *fro::yfp attB*::[$P_{A1/04/03}$-*mCherry*] Δ*pilTU aacc1*::FRT	This study.
AL174	PA14 *fro::yfp attB*::[$P_{A1/04/03}$-*mCherry*] Δ*pilY1 aacc1*::FRT	This study.
AL175	PA14 *fro::yfp attB*::[$P_{A1/04/03}$-*mCherry*] Δ*lasR aacc1*::FRT	This study.
AL452	PA14 P_{fro}*::yfp attB*::[$P_{A1/04/03}$-*mCherry*] Δ*fliC aacc1*::FRT	This study.
AL325	PA14 *fro::yfp attB*::[$P_{A1/04/03}$-*mCherry*] Δ*froR aacc1*	This study.
AL350	PA14 P_{fro}*::yfp attB*::[$P_{A1/04/03}$-*mCherry*] Δ*froI aacc1*	This study.
AL369	PA14 *fro::yfp attB*::[$P_{A1/04/03}$-*mCherry*] *glmS*::[$P_{A1/04/03}$-*froR*]	This study.
AL370	PA14 *fro::yfp attB*::[$P_{A1/04/03}$-*mCherry*] *glmS*::[$P_{A1/04/03}$-*froI*]	This study.

Table S4: Primers used in this study.

Primer	Sequence	Reference
fro-reporter-lred-u1	GCATCCGAAGTCGAGGAGAA	This study.
fro-reporter-lred-l1	cttaatttctcctctttaattctagCTCCTCAGGCCTTACGACTT	This study.
fro-reporter-lred-u2	AAGTCGTAAGGCCTGAGGAGctagaattaaagaggagaaattaag	This study.
fro-reporter-lred-l2	ATTCCCGTTGCATGGTCCGTtgtaggctggagctgcttcg	This study.
fro-reporter-lred-u3	cgaagcagctccagcctacaACGGACCATGCAACGGGAAT	This study.
fro-reporter-lred-l3	GCAATCGGCTTCCTCCAGTA	This study.
pilA-lred-u1	AGGAACTCGGTTTTCTCCGC	This study.
pilA-lred-l1	cgaagcagctccagcctacaGCTCCGAGCGAATGCCGCTAA	This study.
pilA-lred-u2	TTAGCGGCATTCGCTCGGAGCtgtaggctggagctgcttcg	This study.
pilA-lred-l2	GGATATATCAATGGAGAGATACATGattccggggatccgtcgacc	This study.
pilA-lred-u3	ggtcgacggatccccggaatCATGTATCTCTCCATTGATATATCC	This study.
pilA-lred-l3	CGCAGTAGGCGATACCGAAT	This study.
pilB-lred-u1	TACCGGCTTGAGCATTCCAG	This study.
pilB-lred-l1	ggtcgacggatccccggaatCATTGGGAGTGGTCGCATAAGG	This study.
pilB-lred-u2	CCTTATGCGACCACTCCCAATGattccggggatccgtcgacc	This study.
pilB-lred-l2	TTAGTCCTTGGTCACGCGGTTtgtaggctggagctgcttcg	This study.
pilB-lred-u3	cgaagcagctccagcctacaAACCGCGTGACCAAGGACTAA	This study.
pilB-lred-l3	TGGCTTTCAGGGATTCTGTCT	This study.
pilTU-lred-u1	GGAGGTTGGGCAGTTGCTTC	This study.
pilTU-lred-l3	TATCCTCTACGCGACCTACG	This study.
pilY1-lred-u1	ACTGGAAAGCCGTATCAC	This study.
pilY1-lred-l1	CATGCGCTGGCTCCAGTCAG	This study.
pilY1-lred-u2	CATGCACGCCTGTATACCAACTGACTGGAGCCAGCGCATGattccggggatccgtcgacc	This study.
pilY1-lred-l2	AGACGTAAGGGGTTCATGTTCATTTCTCCTCGACGACCCGtgtaggctggagctgcttcg	This study.
pilY1-lred-u3	CGGGTCGTCGAGGAGAAATG	This study.
pilY1-lred-l3	GTTGAATGCCTGGTTAGC	This study.
fliC-lred-u1	AATCGGTCGAGCCTACTCCT	This study.
fliC-lred-l1	cgaagcagctccagcctacaGTCCTGAGCCTGCTGCGCTAA	This study.
fliC-lred-u2	TTAGCGCAGCAGGCTCAGGACtgtaggctggagctgcttcg	This study.
fliC-lred-l2	GGTCCTTTGGAGGAAATCACCATGattccggggatccgtcgacc	This study.
fliC-lred-u3	ggtcgacggatccccggaatCATGGTGATTTCCTCCAAAGGACC	This study.
fliC-lred-l3	CTGCTATCGCGACAGTCTCC	This study.
lasR-lred-l3	GAGAATTCGCCAGCAACCGA	This study.
lasR-lred-u1	TACGCGCCGCCGTTGCAGGC	This study.
Tn7-*froR*-u	ttaaagaggagaaattaagcGTGGCGGCGCCTACCGAC	This study.
Tn7-*froR*-1	aggaattcctcgagaagcttTCAGCATTGGCCGGTCTCC	This study.
Tn7-*froI*-u	ttaaagaggagaaattaagcATGCTGAGTTGCAAGGAACTGGTCGCCC	This study.
Tn7-*froI*-l	aggaattcctcgagaagcttTCAGCGCCGCGCGGCGTC	This study.

Tn7-PA1/04/03-insert-v-l	AAGCTTCTCGAGGAATTCCTG	This study.
Tn7-PA1/04/03-insert-v-u	GCTTAATTTCTCCTCTTTAATTCTAG	This study.
froR-lred-u1	CTGCTGACCCAGTTCTCCAA	This study.
froR-lred-l1	ggtcgacggatccccggaatCACGATCAGTGTTTACGCAGG	This study.
froR-lred-u2	CCTGCGTAAACACTGATCGTGattccggggatccgtcgacc	This study.
froR-lred-l2	TCAGCATTGGCCGGTCTCCTCtgtaggctggagctgcttcg	This study.
froR-lred-u3	cgaagcagctccagcctacaGAGGAGACCGGCCAATGCTGA	This study.
froR-lred-l3	CCCTGCTGGAGAAATATCGGG	This study.
froI-lred-u1	TCATCGGCAGATCGCATACC	This study.
froI-lred-l1	ggtcgacggatccccggaatACTCAGCATTGGCCGGTCTC	This study.
froI-lred-u2	GAGACCGGCCAATGCTGAGTattccggggatccgtcgacc	This study.
froI-lred-l2	GGTACCCCGGCTCAGCGtgtaggctggagctgcttcg	This study.
froI-lred-u3	cgaagcagctccagcctacaCGCTGAGCCGGGGTACC	This study.
froI-lred-l3	AACCTTCCTTGGCCTTCTCG	This study.

Table S5: Plasmids used in this study.

Plasmid	Description	Reference
mini-CTX2	*attB* integration vector	(*29*)
mini-CTX2-$P_{A1/04/03}$-mCherry	Targets constitutively expressed mCherry allele to *attB* site	This study.
pAS03	Vector for generating deletion mutants and fusions	(*16*)
pFLP2	Plasmid expressing FLP2 to recombine FRT sites	(*35*)
pUCP18-RedS	Lambda Red recombineering vector	(*27*)
mini-Tn7-$P_{A1/04/03}$-*froR*	Targets constitutively expressed *froR* to *glmS*	This study.
mini-Tn7-$P_{A1/04/03}$-*froI*	Targets constitutively expressed *froI* to *glmS*	This study.

Supplemental References

27. Lesic, B. & Rahme, L.G. Use of the lambda Red recombinase system to rapidly generate mutants in *Pseudomonas aeruginosa*. *BMC Molecular Biology* **9**, 20 (2008)
28. Choi, K.H. & Schweizer, H.P. mini-Tn7 insertion in bacteria with single attTn7 sites: example *Pseudomonas aeruginosa*. *Nature Protocols* **1**,153-161 (2006)
29. Hoang, T.T., Kutchma, A.J., Becher, A., & Schweizer, H.P. Integration-proficient plasmids for *Pseudomonas aeruginosa*: site-specific integration and use for engineering of reporter and expression strains. *Plasmid* **43**, 59-72 (2000)
30. Langmead, B. & Salzberg, S.L. Fast gapped-read alignment with Bowtie 2. *Nature Methods* **9**, 357-359 (2012)
31. Kim, M.K., Ingremeau, F., Zhao, A., Bassler, B.L., & Stone, H.A. Local and global consequences of flow on bacterial quorum sensing. *Nature Microbiology* **1**, 15005 (2016)
32. Koch, M.D. & Shaevitz, J.W. Introduction to Optical Tweezers. *Methods in Molecular Biology* **1486**, 3-24 (2017)
33. Simon, R., Quandt, J., & Klipp, W. New derivatives of transposon Tn5 suitable for mobilization of replicons, generation of operon fusions and induction of genes in gram-negative bacteria. *Gene* **80**, 161-169 (1989)
34. Rahme, L.G.*, et al.* Common virulence factors for bacterial pathogenicity in plants and animals. *Science* **268**, 1899-1902 (1995)
35. Hoang, T.T., Karkhoff-Schweizer, R.R., Kutchma, A.J., & Schweizer, H.P. A broad-host-range Flp-FRT recombination system for site-specific excision of chromosomally-located DNA sequences: application for isolation of unmarked *Pseudomonas aeruginosa* mutants. *Gene* **212**, 77-86 (1998)